

SYNTHESIS OF HIGH-ACTIVITY C AEROGELS-BASED g-C₃N₄ PHOTOCATALYSTS DERIVED BY THE POLYMERIZATION OF PF

X. LI^a, Q. YU^{b,*}, Y. TAO^b

^a*School of Mechanical Engineering, Anhui University of Science and Technology, Huainan 232001, PR China*

^b*Department of Materials Science and Engineering, Anhui University of Science and Technology, Huainan 232001, PR China*

This paper details the synthesis of high-activity carbon (C) aerogels-based g-C₃N₄ catalysts for photocatalytic degradation under visible light. We seal and heat a mixture of phenol (P), ZnCl₂ and g-C₃N₄ solvated by formaldehyde, obtaining the mixture of an intimate interaction between phenol-formaldehyde (PF) and g-C₃N₄ as precursor of C aerogels-based g-C₃N₄. The post thermal treatment results in not only carbon-doped g-C₃N₄ which improve the π -conjugation system to profit the separation of photo-induced carrier, but also obtaining C aerogels which possess high surface area. The resulted C aerogels-based g-C₃N₄ catalysts shown high adsorption capacity (78 mg/g), broadened light absorption, improved photoelectrochemical performance and higher photocatalytic properties compared with pristine g-C₃N₄.

(Received February 23, 2018; Accepted June 8, 2018)

Keywords: C aerogels-based g-C₃N₄, Phenol-formaldehyde, Carbon doping, Surface area, Photocatalytic properties

1. Introduction

Graphitic carbon nitride (g-C₃N₄), as a organic semiconductor, has attracted considerable attention in photocatalytic degradation because of its suitable band structure, nontoxicity, abundance and highly physicochemical stability.[1,2] However, its development has disadvantages such as faster recombination of the electron-hole pairs, poor surface area, low visible light absorption, and seriously agglomerated in most solvents caused by the strong van der Waals attractions between sp² carbon atoms.[3,4]

To overcome these short comings, previous researchers have employed strategies such as doping, nanostructure engineering, coupling with other materials, and introducing electrostatic repulsion among adjacent layers to achieve stable dispersion.[5-7] Yet most studies only consider one aspect of disadvantages, and ignore the other aspects. For example, Bu et al.[8] prepare uniformly dispersed g-C₃N₄ solution by treating it with oxygen plasma. This method on the one hand enhance the effective interaction between photocatalysts and target molecules, while on the other hand narrow light absorption, enhance the difficulty of recycling. Therefore, there is still an urgent call for a novel and efficient method to interconnect various aspects of performance.

As catalyst supports, porous carbon aerogels have drawn highly attention due to its large surface area, easy recycle, superior adsorption efficiency, and fast material transfer through broad interpenetrated channels.[9,10] But beyond that, carbon-based materials, using as coupling in photocatalysts, can also enhance the photoelectrochemical properties and conductivity of catalysts.[11] It is therefore desirable to develop photocatalysts that combine carbon aerogels with g-C₃N₄ resulting in the superior combination property, such as improving adsorption capacity, suppressing recombination of photogenerated charges, easy recycle, and high carbon-based isolation to prevent agglomerated of g-C₃N₄ in solvents.

In this work, the C aerogels-based g-C₃N₄ photocatalysts were prepared based on Fig. 1. The raw materials for C aerogels are phenol and formaldehyde. Firstly, formaldehyde segregates the stacked g-C₃N₄, obtained solvated g-C₃N₄ by forming hydrogen bonds. After adding phenol and

*Corresponding author: yuqingbo007@163.com

ZnCl₂, the polymerization occurs in Teflon-lined autoclave. The obtained sample is the mixture of an intimate interaction between phenol-formaldehyde (PF) and g-C₃N₄. In addition the g-C₃N₄ insulated by PF in mixture, which prevent the agglomerated of g-C₃N₄. Then, the mixture was heated under flowing nitrogen atmosphere at 600 °C for 1.5h. In the formed C aerogels-based g-C₃N₄ photocatalysts, there are two processes. One, the C aerogels produced from PF annealing using ZnCl₂ as foaming agent and porogen,[12] which can improve the adsorption capacity of photocatalysts. Second, the g-C₃N₄ may be incorporated with aromatic heterocycles in C by annealing, because of the π - π interaction between PF and g-C₃N₄.

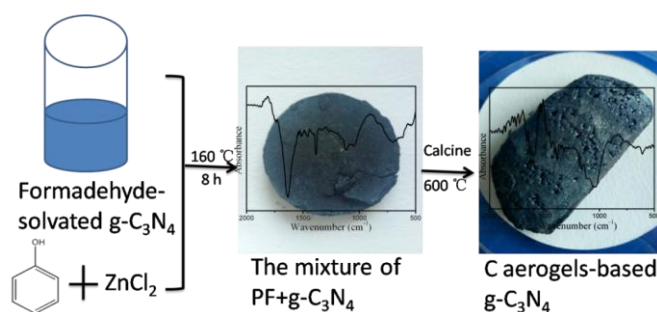


Fig. 1. The process of the C aerogels-based g-C₃N₄ photocatalyst.

The PF-derived carbon (C) atoms repair the nitrogen (N) vacancies in g-C₃N₄. The C atom in triazine units and the attaching aromatic heterocycles may extend the delocalization of electrons in the π -conjugation system, promoting charge separation and transportation.[13] After purifying in 1 M HCl, the C aerogels-based g-C₃N₄ possesses a high surface area (800 m² g⁻¹). Thus, the obtained photocatalysts may exhibit high photocatalytic activity because of bifunctional effect owing to C aerogels and higher dispersion g-C₃N₄ in C-based, such as extending π -conjugation, large surface area, high transmission of photogenerated charges, and preventing agglomerated of g-C₃N₄ in solvents.

2. Experimental

2.1. Synthesis of C aerogels-based g-C₃N₄ catalysts

The g-C₃N₄ is prepared by heating dicyandiamide at 550 °C for 4h.[14] After that, we mixed 1.5 mL formaldehyde and 0.3 g g-C₃N₄ by ultrasonic to obtain solvated g-C₃N₄ by forming hydrogen bonds. Then, the 0.491 g phenol and 6 g zinc chloride (ZnCl₂) were added to yield viscous sol. The sol was transferred to sealed autoclave, followed by heating at 160 °C for 8 h. The geted mixture of phenol-formaldehyde (PF) and g-C₃N₄ were dried at 100 °C and heated to 600 °C at a rate of 2.5 °C min⁻¹. After keeping this temperature for 1.5 h, the C aerogel-based g-C₃N₄ was purified in 1M HCl several times, and then filtered and dried. The obtained sample is signed as C aerogels-based g-C₃N₄(0.3). In order to compare the effect of the concentration in g-C₃N₄, variable quantity g-C₃N₄ (0.1 g and 0.2 g) were added, replacing 0.3 g g-C₃N₄ in reaction, while the other process is unchanged. The obtained samples is denoted as C aerogels-based g-C₃N₄(0.1) and C aerogels-based g-C₃N₄(0.2), respectively. In addition, we have calcined g-C₃N₄ again at 600 °C for 1.5 h. The sample is signed as g-C₃N₄(a).

2.2. Characterization

A UV-vis spectrophotometer (Varian CARY 100, USA) is use to characterize the UV-vis diffuse reflection spectra. The structure of the samples was measured using X-ray diffraction (XRD Rigaku RINT2000 diffractometer), Fourier transform spectrophotometer (FTIR), and X-ray photoelectron spectra (XPS Thermo ESCALAB 250). The morphology of the samples was characterized by field-emission scanning electron microscopy (SEM). The Q2000 thermogravimetric analyzer was used as thermo gravimetric analysis (TGA) in argon gas. The CHI 660E electrochemical workstation was using as electrochemical measurements by three electrode

cells.

2.3. Adsorption measurements

Methylene blue (MB) solutions of 31 and 62 μM concentrations were obtained in aqueous medium. 3 mg of sample was put in MB solutions and stayed for over 40 min to saturation. The adsorption capacity, q_e (mg g^{-1}), can be calculated according to the equation (1);

$$q_e = \frac{c_0 - c_t}{m} \times V \quad (1)$$

where C_0 is MB concentration (mg L^{-1}) at the start, and C_t is the concentration after contact time t (min). V and m correspond to the solution volume and the amount of adsorbent added.

The photocatalytic activity

The photocatalytic ability of the samples were tested by photodegradation of MB under visible light irradiation (>420 nm). In detail, 3 mg sample was put in MB (62 μM) aqueous solution. After saturated adsorption, UV-vis spectrophotometer (664 nm) is use to examine the degradation of MB solution.

3. Results and discussion

Fig. 2 displays the FTIR spectra of the samples. Compared with the C specimens (Fig. 2-2), the C aerogels-based $g\text{-C}_3\text{N}_4$ showed additional peak at 805 cm^{-1} (Fig. 2-1), which equivalent of the stretching vibration mode of the tri-s-triazine units in $g\text{-C}_3\text{N}_4$ (Fig. 2-3). The band at 1637 cm^{-1} equivalent of the breathing mode of C=C (Figure 2-2), become broad band at $1637\text{-}1588\text{ cm}^{-1}$ (Fig. 2-1). This FTIR analysis confirmed not only the existence of $g\text{-C}_3\text{N}_4$ in C aerogels-based $g\text{-C}_3\text{N}_4$, but also an interaction between C aerogels and $g\text{-C}_3\text{N}_4$.

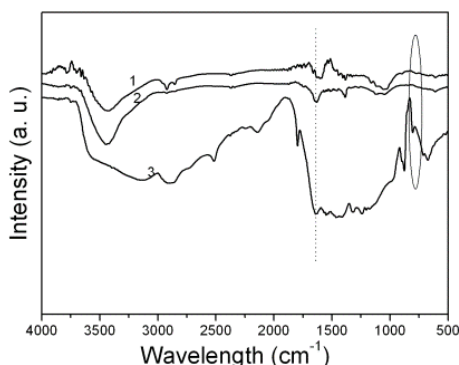


Fig. 2. FTIR spectra of (1) C aerogels-based $g\text{-C}_3\text{N}_4$, (2) C and (3) $g\text{-C}_3\text{N}_4$.

XPS analysis of $g\text{-C}_3\text{N}_4$ and C aerogels-based $g\text{-C}_3\text{N}_4$ is displayed in Fig. 3. From Fig. 3a and Fig. 3c, the constituent of C 1s spectra is 284.7 eV, 285.2 eV, 286.4 eV and 288.5 eV for graphitic C=C or the cyano-group, adventitious carbon, C-NH₂ species and SP²-hybridized carbon, respectively. The high-resolution N 1s spectra (Fig. 3b and 3d) and the constituent peaks are located at 399.4 and 400.9 eV for N atoms in N-(C)₃ or sp²-bonded N in triazine system and the end of amino groups, respectively.[15,16] The peaks intensity of 284.7 eV and 285.2 eV in C 1s spectra (Fig. 3c) are increased comparing with Fig. 3a, while the peak at 397.7 eV (N 1s Fig. 3d) is decreased in C aerogels-based $g\text{-C}_3\text{N}_4$ sample comparing with Fig. 3b. In addition, the C/N ratio estimated from the XPS analysis implied an increase from 1.4 for $g\text{-C}_3\text{N}_4$ to 45.9 for C aerogels-based $g\text{-C}_3\text{N}_4$. The results indicated the deficiency of N in C aerogels-based $g\text{-C}_3\text{N}_4$ prompted by calcinations process and subsequent in situ doping of carbon from the residue of phenol-formaldehyde resin (PF) burned out.[17]

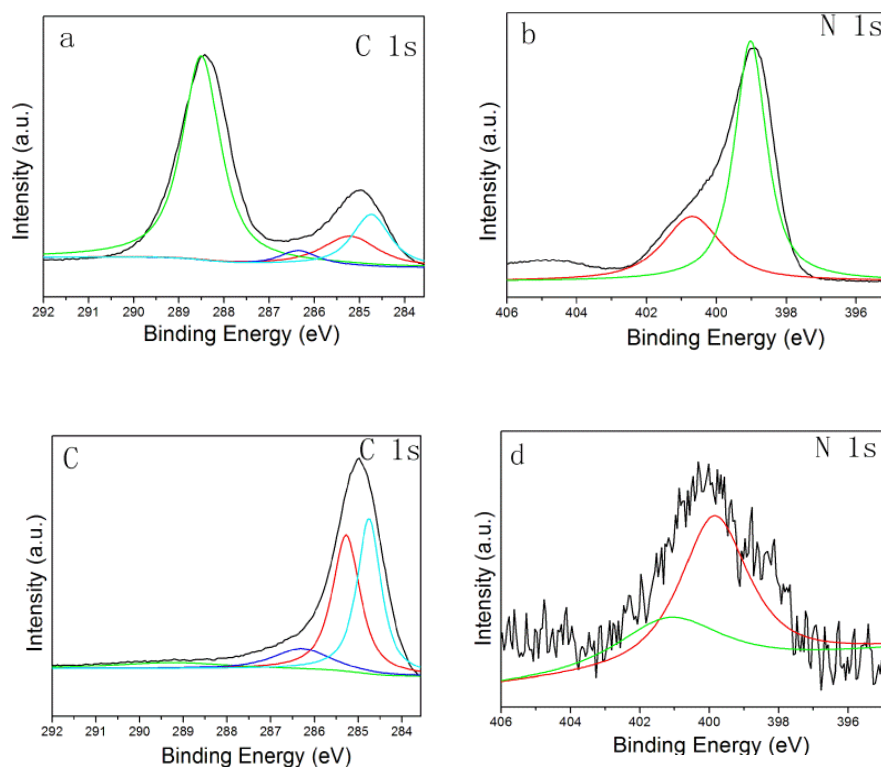


Fig. 3. XPS patterns (a) C 1s and (b) N 1s of $g\text{-C}_3\text{N}_4$ and (c) C 1s and (d) N 1s of C aerogels-based $g\text{-C}_3\text{N}_4$.

We further examined the doping of carbon in C aerogels-based $g\text{-C}_3\text{N}_4$ by the degradation curve and XRD analysis. From Fig. 4a, both showed similar XRD curve for the $g\text{-C}_3\text{N}_4$ and $g\text{-C}_3\text{N}_4$ (a). The stacking peak of conjugated aromatic systems is exhibited at around 27.4° . It conform the $g\text{-C}_3\text{N}_4$ calcined again at 600°C do not change the stacking structure. However, the C aerogels-based $g\text{-C}_3\text{N}_4$, obtained by calcinating the mixture of PF and $g\text{-C}_3\text{N}_4$ at 600°C , have similar XRD curve with C (Fig. 4b). It has not the XRD peak (002) at around 27.4° . The reason may be the structural damage in $g\text{-C}_3\text{N}_4$ causing by doping of carbon by calcination of the PF, which act as in turn the crosslinking of PF, improved crosslinking density.

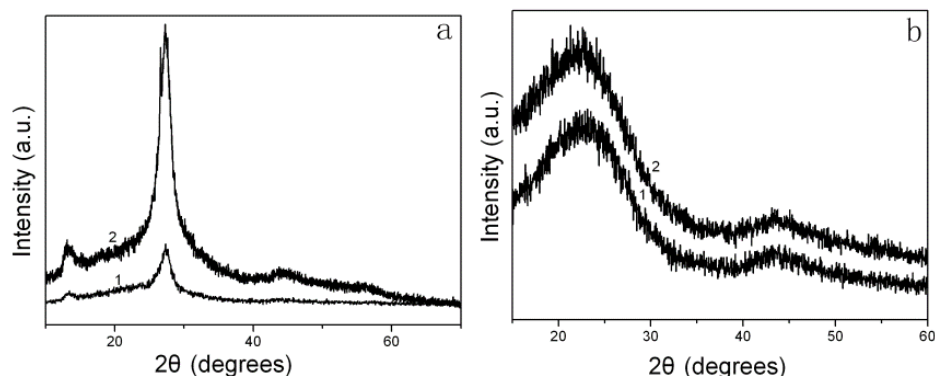


Fig. 4. XRD spectra of (a) $g\text{-C}_3\text{N}_4$ (1) and $g\text{-C}_3\text{N}_4$ (a); (b) C (1) and C aerogels-based $g\text{-C}_3\text{N}_4$ (2).

From Fig. 5a, both of the TGA followed similar weight loss pattern for PF, $g\text{-C}_3\text{N}_4$ and the mixture of PF and $g\text{-C}_3\text{N}_4$. However, the mixture of PF and $g\text{-C}_3\text{N}_4$ fabricated by polymerization

(Fig. 5a-1), shows a slow weight loss comparing with PF and $g\text{-C}_3\text{N}_4$ (Fig. 5a-2 and 5a-3), implying thermally more stable. The DTA curve showed a sharp peak at 655°C , 679°C and 526°C for the mixture of PF and $g\text{-C}_3\text{N}_4$, $g\text{-C}_3\text{N}_4$ and PF, respectively (Fig. 5b). The decomposition for the mixture of PF and $g\text{-C}_3\text{N}_4$ occurs at higher temperature compared with PF, implying the superior thermal stability for the main chains of PF.[18] Thus it can be interpreted that the residue of PF burn out improve in situ doping of carbon in C aerogels-based $g\text{-C}_3\text{N}_4$, which cause more crosslinking in interchain of PF, hence an increase in stability. This is consistent with the above XRD analysis.

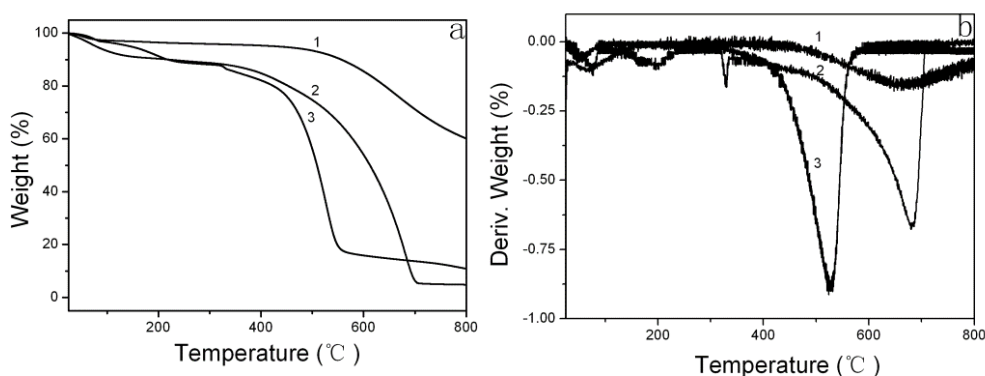


Fig. 5. TGA (a) and DTG (b) curves of the mixture of PF and $g\text{-C}_3\text{N}_4$ (1), $g\text{-C}_3\text{N}_4$ (2) and PF (3).

In fact, the replacement of bridging nitrogen by carbon due to doping, can create large delocalized π bonds, which enhances the electrical conductivity and impedes the electron hole recombinations. All of those may provide novel optoelectronic properties. The UV-vis spectra of the sample is shown in Fig. 6a, the C aerogels-based $g\text{-C}_3\text{N}_4$ reveals broad light absorption intensity in the whole regions comparing with $g\text{-C}_3\text{N}_4$, which is a typical behavior of carbon-based materials.[19] It is attributed to narrower gap of the sp^2 carbon cluster embedded in C, which possess the superior light absorption in the entire wavelength.[20]

The photoelectrochemical properties are investigated by I-V curves (Fig. 6b). The photocurrent density of C aerogels-based $g\text{-C}_3\text{N}_4$ shows higher at potentials from -2 to 2 V than that of pristine $g\text{-C}_3\text{N}_4$. These results illustrate that the unique structure increase the contact area, which shorten the diffusion distance of electron shuttling between reactive sites, suppresses recombination ration of photoinduce electron-hole. In addition, the C in C aerogels-based $g\text{-C}_3\text{N}_4$ increases the lightharvesting capability, which enhancement the ability of photogenerated electron-hole pairs.

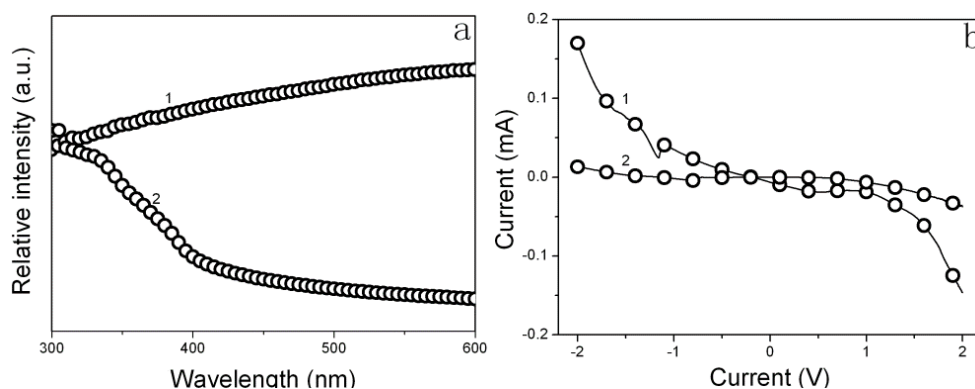


Fig. 6. UV-vis spectra (a) and I-V curves of C aerogels-based $g\text{-C}_3\text{N}_4$ (1) and $g\text{-C}_3\text{N}_4$ (2).

Fig. 7 display SEM images of $g\text{-C}_3\text{N}_4$, C and C aerogels-based $g\text{-C}_3\text{N}_4$. From Fig. 7a, $g\text{-C}_3\text{N}_4$ consisted of the stacking sheets. And the carbon obtained by calcinations of PF, is composed of adhesion spheres (Fig. 7b). After calcination of the mixture of PF and $g\text{-C}_3\text{N}_4$ at 600°C , the

morphology of obtained C aerogels-based $g-C_3N_4$ is different from $g-C_3N_4$ and C, which consist of separate spheres coated by bulk $g-C_3N_4$ (Fig. 7c). The $g-C_3N_4$ in C aerogels-based $g-C_3N_4$ is smaller than the original $g-C_3N_4$, indicating that annealing on the PF that adhered to the $g-C_3N_4$ may have modified polymeric melon units to reduce substantially the size[16].

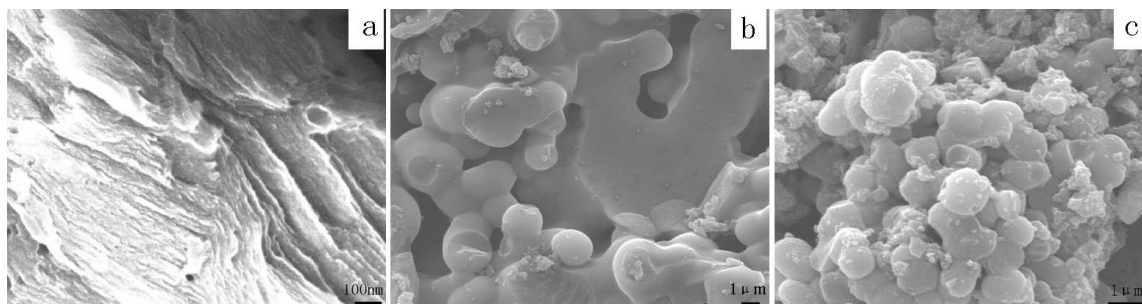


Fig. 7. SEM of $g-C_3N_4$ (a), C (b) and C aerogels-based $g-C_3N_4$ (c).

In addition, this structure of separate spheres can increase the surface area of the C aerogels-based $g-C_3N_4$ photocatalyst, which probably improve the adsorption capacity. It is investigated by estimating the samples in the MB concentrations changing from 31 to 62 μM (Fig. 8a). The adsorption capacity increases when the MB concentration increases both of the two samples. However, no matter what the MB concentration change, the adsorption capacity of C aerogels-based $g-C_3N_4$ is higher than pristine $g-C_3N_4$. It is a universal phenomenon that the π -conjugate in samples induce the adsorption of π -conjugated carbon clusters in MB. But, the enhanced adsorption capacity in C aerogels-based $g-C_3N_4$ may be caused by the enhanced π -conjugate produced by the carbon doping in $g-C_3N_4$. The C atoms take place of the bridging N atoms. Then, enlarging delocalized π bonds are induced among the substituted C and the hexatomic rings, improving the adsorption capacity in C aerogels-based $g-C_3N_4$. [21] In addition, it is important that C aerogels produce high surface area.

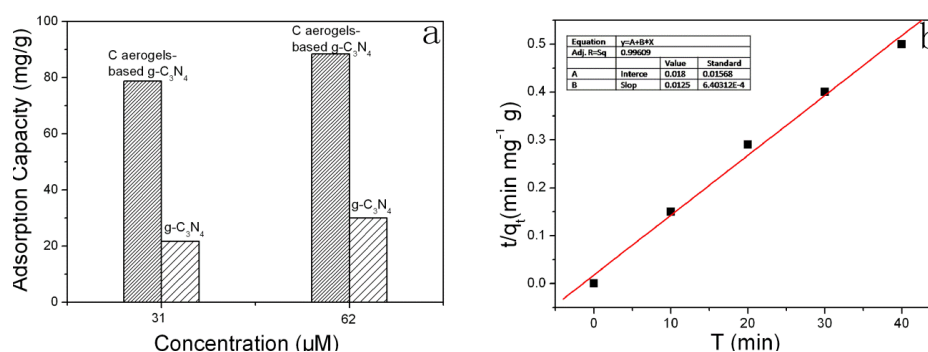


Fig. 8. (a) Adsorption capacity of samples; (b) Pseudo second order kinetics of C aerogels-based $g-C_3N_4$.

The rate of adsorption followed pseudo-second order kinetics where the linear form is represented as Eq. 2.

$$\frac{t}{q_t} = \frac{1}{q_e} \times t + \frac{1}{K_2 \times q_e^2} \quad (2)$$

where, q_t ($mg\ g^{-1}$) is the amount of MB adsorption at the contact time of t on per unit mass of C aerogels-based $g-C_3N_4$. K_2 is the pseudo-second order rate constants. The typical pseudo-second

order kinetics plot is showed in Fig. 8b. The details of pseudo-second order kinetics are summarized in Table 1. The value of regression correlation coefficient (R_2) is close to 1. The experimentally determined value of q_e is comparable with the estimated q_e value calculated by this model. So the pseudo-second order kinetics is suited for the adsorption of MB on the C aerogels-based g-C₃N₄. This result supply the higher adsorption capacity in C aerogels-based g-C₃N₄ (78.8 mg g⁻¹) can be due to enhanced π - π interaction produced by the carbon doping in g-C₃N₄ and high surface area owing to C aerogels. The enhanced adsorption is an important factor for photocatalytic efficiency.

Table 1. Summary of the parameters of pseudo second order kinetics.

concentration	31.3 μ M
kinetics	Pseudo-second order
r^2	0.99609
K_2	0.0087
q_e (calculated)	80
q_e (experimental)	78.8

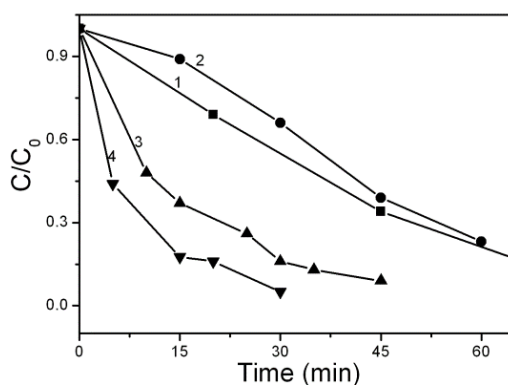


Fig. 9. Photocatalytic degradation of g-C₃N₄ (1), C aerogels-based g-C₃N₄(0.1) (2), C aerogels-based g-C₃N₄(0.2) (3), C aerogels-based g-C₃N₄(0.3) (4).

The photocatalytic experiments of the as-synthesized sample were carried out under visible light irradiation using MB as a model pollutant. From Fig. 9, the C aerogels-based g-C₃N₄ (0.3) shows higher photocatalytic degradation in comparison with pristine g-C₃N₄, due to not only small amount doped carbon and high surface area caused by C aerogels, but also preventing agglomerated of g-C₃N₄ in solvents. However, the photocatalytic degradation decrease when the concentration of C increase without limit. Especially, the C aerogels-based g-C₃N₄(0.1) shows lower photocatalytic degradation comparing with pristine g-C₃N₄. The reason may be too few concentration of g-C₃N₄.

4. Conclusions

In conclusion, we developed a facile route to prepare C aerogels-based g-C₃N₄, which possess suppressing recombination of photogenerated charges due to enhancing π -conjugation system, improving adsorption capacity owing to C aerogels structure, enhancing the effective interaction between photocatalysts and target molecules caused by separation of g-C₃N₄ in C aerogels. The process in preparing the mixture of PF and g-C₃N₄ play the key role in doped carbon process, in which formaldehyde molecules were anchored on g-C₃N₄ to segregate the sheet and flow polymerization to attach PF with g-C₃N₄ by π -conjugation. In annealing treatment, on the one hand

PF-derived carbon (C) atoms repair the nitrogen (N) vacancies in g-C₃N₄, while on the other ZnCl₂ adding in process of preparing mixture of PF and g-C₃N₄ was used as foaming agent and porogen, and crucial to directly obtain the C aerogels.

The use of the devised method not only increase the π -conjugation system and the surface area of C aerogels-based g-C₃N₄, but also effectively separate g-C₃N₄ in C aerogels, which facilitated charge separation, higher adsorption capacity, and available material contact. The catalyst show high photocatalytic degradation. This finding exhibits the high potential of extending the π -conjugation systems and improving surface areas by PF annealing, and offer an effective path for the preparation of highly active photocatalysis.

This work was supported by the National Nature Science Foundation of China (21401001), Postdoctoral Science Foundation of China (2015M571913), Anhui Province Natural Science Foundaion (160808085MB25) and Postdoctoral Fund in Anhui (2016B090 and 2016B108)

References

- [1] J. Zhu, P. Xiao, H. Li, S. A. C. Carabineiro, *ACS Appl. Mater. Interfaces* **6**, 16449 (2014).
- [2] N. Cheng, J. Tian, Q. Liu, C. Ge, A. H. Qusti, A. M. Asiri, A. O. Al-Youbi, X. Sun, *ACS Appl. Mater. Interfaces* **5**, 6815 (2013).
- [3] E. G. Gillan, *Chem. Mater.* **12**, 3906 (2000).
- [4] R. Lv, T. Cui, M. Jun, Q. Zhang, A. Cao, D. Su, Z. Zhang, S. Yoon, J. Miyawaki, I. Mochida, F. Kang, *Adv. Funct. Mater.* **21**, 999 (2011).
- [5] A. Reddy, A. Srivastava, S. Gowda, H. Gullapalli, M. Dubey, P. Ajayan, *ACS Nano*. **4**, 6337 (2010).
- [6] Q. Yu, S. Guo, X. Li, M. Zhang, *Mater. Technol.* **3**, 172 (2014).
- [7] Q. Yu, X. Li, L. Zhang, X. Wang, Y. Tao, X. Wang, *J. Polym. Mater.* **4**, 417 (2015).
- [8] X. Bu, J. Li, S. Yang, J. Sun, Y. Deng, Y. Yang, G. Wang, Z. Peng, P. He, X. Wang, G. Ding, J. Yang, X. Xie, *ACS Appl. Mater. Interfaces* **8**, 31419 (2016).
- [9] G. Hao, W. Li, D. Qian, G. Wang, W. Zhang, T. Zhang, A. Wang, F. Schgth, H. Bongard, A. Lu, *J. Am. Chem. Soc.* **133**, 11378 (2011).
- [10] B. Zeng, W. Zeng, *Dig. J. Nanomater. Bios.* **1**, 215 (2017).
- [11] F. Guo, W. Shi, W. Guan, H. Huang, Y. Liu, *Sep. Purif. Technol.* **173**, 295 (2017).
- [12] Z. Yu, G. Li, N. Fechner, N. Yang, Z. Ma, X. Wang, M. Antonietti, S. Yu, *Angew. Chem. Int. Ed.* **55**, 14623 (2016).
- [13] Y. Zhou, L. Zhang, W. Huang, Q. Kong, X. Fan, M. Wang, J. Shi, *Carbon*. **99**, 111 (2016).
- [14] Q. Yu, X. Li, M. Zhang, *Micro Nano Lett.* **1**, 1 (2014).
- [15] L. Ma, H. Fan, K. Fu, S. Lei, Q. Hu, H. Huang, *ACS Sustainable Chem. Eng.* **5**, 7093(2017).
- [16] P. Chuang, K. Wu, T. Yeh, H. Teng, *ACS Sustainable Chem. Eng.* **4**, 5989 (2016).
- [17] S. Panneri, P. Ganguly, M. Mohan, B. N. Nair, A. A. P. Mohamed, K. G. Warriar, U. S. Hareesh, *ACS Sustainable Chem. Eng.* **5**, 1610 (2017).
- [18] F. Deng, L. Min, X. Luo, S. Wu, S. Luo, *Nanoscale.* **5**, 8703 (2013).
- [19] F. Z. Su, S. C. Mathew, G. Lipner, X. Z. Fu, M. Antonietti, S. Blechert, X. C. Wang, *J. Am. Chem. Soc.* **132**, 16299 (2010).
- [20] D. Pan, J. Zhang, Z. Li, C. Wu, X. Yan, M. Wu, *Chem. Commun.* **46**, 3681 (2010).
- [21] G. Dong, K. Zhao, L. Zhang, *Chem. Commun.* **48**, 6178 (2012).